A Proposal of a Heat Input Model, for Heating Correction, on Welded Steel Structural Members

Guan Xiaoyu, Tokumaru Yujiro, Hirohata Mikihito*

Graduate School of Engineering, Osaka University
2-1, Yamada-oka, 5650871, Suita, Osaka, Japan;
x-guan@civil.eng.osaka-u.ac.jp; y-tokumaru@civil.eng.osaka-u.ac.jp;
hirohata@civil.eng.osaka-u.ac.jp (corresponding author)

Mukawa Satoshi, Okada Seiji

IHI Infrastructure Systems, 3-17-12, Shibaura, Minato-ku, 1080023, Tokyo, Japan; mukawa7877@ihi-g.com; okada0269@ihi-g.com

Abstract: A series of experiments and analyses were conducted for evaluating a simple heat input model, for heating correction on welded steel structural members. The heating experiment on steel plates, with different thicknesses, was simulated using thermal elastic–plastic analysis. The temperature histories, deformations and residual stresses of plates could be simulated by the simplified heat source model, proposed in this study. The applicability of the heat source model was verified, by simulating the heating correction for T-shaped fillet welded joints.

Keywords: Welding; Steel structures; Deformation; Heating correction; Finite element analysis

1 Introduction

Welding is widely used to manufacture factory and on-site joints as a joining method for the fabrication of steel structural members. Compared with other joining methods, such as high-strength bolting, welding has the advantages of greater design freedom, higher workability in narrow spaces, and the ability to reduce the weight of structures. However, there are drawbacks, such as deformation due to heat input from the weld, generation of residual stress, and the risk of defects and cracks in the weld. Welding deformation adversely affects assembly accuracy and strength; therefore, if the deformation exceeds the allowable value, it must be corrected.

There are several correction methods, such as fixing the shrunken part using a hammer, heating the stretched part with gas burners, and correcting the deformation using the temperature difference between the front and back surfaces of the member (heating correction), etc. Among these methods, heating correction is generally used owing to its high workability. The heating position and time depend on the experience of the skilled technicians. With the reduction in the number and aging of technicians, the difficulty of transferring technical expertise to the next generation of technicians has become an important issue.

Many studies have been conducted on the relationship between heat input conditions and deformation, when steel structural members are heated with gas burners [1] [2]. The heating correction of welded assembly parts is similar to that of the bend processing technology [3]. However, the size and curvature of the deformation for the heating correction of welded members differ from those of the bending operation of hull structures. The estimation of the relationship between the heat input condition and correction effects using a numerical simulation based on the finite element method can contribute to the efficiency and automation of heating correction work. A method for precisely modeling the heat input owing to a gas flame, which simulates the heat input for plate bending using the finite element method, has been proposed [4-5].

However, for the heating correction simulation of large, welded assembly parts, a simpler and more versatile heat input model is necessary.

In this study, heating experiments and simulations were performed to develop a simple heat input model based on a previous study [6]. Heating-correction experiments and simulations of T-joint members were conducted to validate the proposed model. This study contributes to the establishment of an effective simulation method for reproducing the heating-correction process. The heat input model introduced in this study is a simple and versatile model that can be used for the heating correction simulation of welded assembly parts, thus being potentially useful in various engineering areas.

2 Experiment

2.1 Specimen

To simulate the heating correction process in this study, a thermal elastic–plastic analysis was performed using the finite element method. Moreover, to propose a simple heat input model of a gas flame for heating correction, basic gas-flame heating experiments and simulations were conducted.

The steel plates used for the experiment were square, 200mm on each side. The plate thicknesses were 9, 12, and 25 mm, respectively. Figure 1 shows the shapes and dimensions of the specimens. Six specimens were used. Two specimens of different thicknesses were prepared. The plate was made of general structural steel SM400A, as specified by JIS G3106. Table 1 lists the mechanical properties of the materials, including their yield strength, tensile strength, and elongation, as illustrated in the mill test reports. The specimens were annealed before heating to remove the initial residual stress caused by rolling.

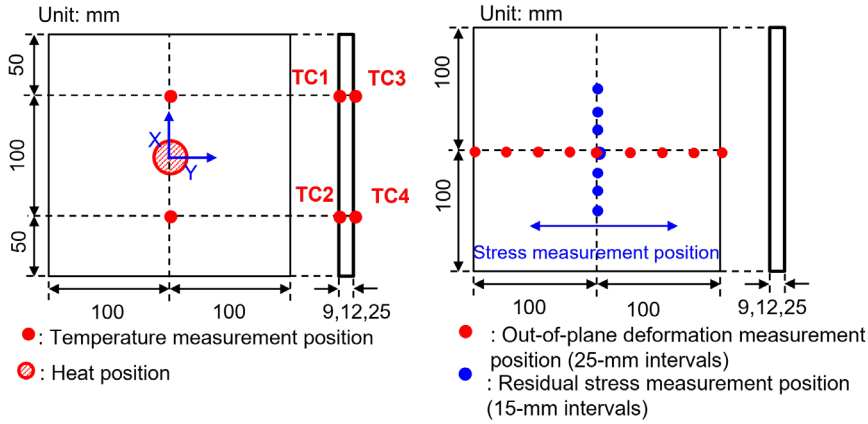

Figure 1

Shapes and dimensions of steel plate specimens and measurement positions of (a) temperature and (b) out-of-plane deformation and residual stress on the steel plate specimens

Table 1

Mechanical properties of materials for steel plate specimens

Thickness (mm)	Yield strength (N/mm^2)	Tensile strength (N/mm^2)	Elongation (%)
9	333	442	30
12	294	422	34
25	301	442	33

2.2 Experimental Procedure

According to the Specifications for Highway Bridges (II Steel Bridges/Steel Members Edition) [7], the surface temperature of steel materials in heating correction should be below 750 °C for tempered steel to suppress changes in the metal structure of steel materials. In this experiment, the target temperature of the heated surface of the steel plate by the gas burner was set at 500–600 °C. The burner used propane as the fuel and oxygen as the oxidizer; the flame length was 70 mm,

and the gas flame temperature was 1,500–1,800 °C. The heat input to the specimen was located at the center of one of its sides, and heating was performed for 20 s. The gas flow velocity was adjusted appropriately while the flame conditions were checked. After heating, the specimens were allowed to cool naturally.

To measure the temperature history of the specimens, thermocouples were attached at two locations on the front and back surfaces (front surface: TC1 and TC2; back surface: TC3 and TC4). Figure 1 (a) shows the positions of the thermocouples. The thermocouples were of K-type used for relatively high-temperature ranges. In addition, the central temperatures of the front and back surfaces of the specimens were measured using the InfRec R450Pro infrared camera. The temperature history during the heating process was measured using thermocouples and an infrared camera, whereas that during the cooling process was measured only using thermocouples.

Figure 2 shows the installation and heating conditions of the specimens. The specimens were fixed using a magnet during heating. After heating, the specimens were removed from the burner installation table and left unrestrained during cooling. As the specimen and thermocouples were covered by a gas flame jet on the surface during heating, the temperature of the specimen could not be measured accurately using an infrared camera and thermocouples at the front surface. Therefore, in this experiment, the temperature history of the back surface of the specimen was used as the simulation target, as described later.

Unit: mm

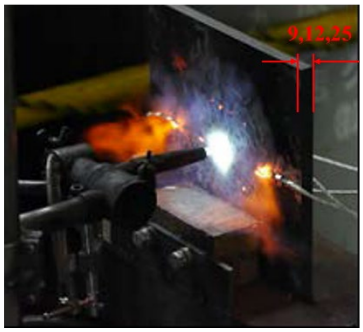

Figure 2
An image of heating experiment on steel plate specimen

After heating and cooling, the out-of-plane deformation was measured using a dial gauge at nine points (25-mm intervals) on the centerline in the horizontal direction of the specimen. The out-of-plane deformation was also measured before heating, and the out-of-plane deformation due to heating was obtained as the difference in deformation before and after heating (Figure 1 (b)). The residual stress was measured via X-ray diffraction (μ-X360s, Pulstec Industrial Co., Ltd.) at seven points (15-mm intervals) on the centerline in the vertical direction of the steel plate (Figure 1 (b)). The radiation source for the X-ray diffraction method was chromium.

The collimator diameter was 1.0 mm. The voltage and current of the X-ray tube were 30 kV and 0.5 mA, respectively.

3 Flame Simulation by Thermal Fluid Analysis

3.1 Analysis Method

To construct a heat input model for thermal elastic–plastic analysis (described later), thermal fluid analysis was performed to examine the heat flow velocity distribution affecting the range of heat input to the steel plate owing to the gas flame.

Previous studies have shown that the shape of the heat flux distribution can be classified according to the ratio of the burner diameter B (mm) to the distance H (mm) from the heated steel material [8]. In this study, the diameter was 14mm, and the distance between the specimen and gas burner was 20mm. A feature of the heat flux distribution when $0.5 < H / B < 7$ is that the maximum temperature appears outside the heating center. In addition, the flame temperature directly above the steel plate significantly affects the determination of the heat input to the steel plate. The temperature directly above the steel plate is proportional to the heat input [9]. In this study, to determine the maximum point of the heat flux distribution, the temperature distribution directly above the steel plate was calculated using thermal fluid analysis [10] [11] based on the approximate solution method, as shown below.

The basic equations for a turbulent combustion field in an axisymmetric two-dimensional plane are the continuity equation, two-way Navier–Stokes equation, and conservative scalar equation shown in Equations (1), (2) and (3), respectively. To introduce a conserved scalar quantity, the ratio of the Lewis number (temperature diffusion coefficient and concentration diffusion coefficient) was set to 1, and the fluid was assumed to be incompressible by the low Mach approximation.

$$\frac{\partial u}{\partial x} + \frac{\partial v}{\partial y} = 0 \tag{1}$$

$$\frac{\partial V}{\partial t} + u\frac{\partial V}{\partial x} + v\frac{\partial V}{\partial y} = \frac{\partial p}{\partial x} + \frac{1}{Re}\left(\frac{\partial^2 u}{\partial x^2} + \frac{\partial^2 v}{\partial y^2}\right) \tag{2}$$

$$\frac{\partial T}{\partial x} + \frac{\partial}{\partial x}(VT) = a\frac{\partial T}{\partial x \partial y} \tag{3}$$

where V is the velocity (m/s), u and v are the velocity components in the x and y directions (m/s), respectively, t is time (s), p is pressure (Pa), Re is the Reynolds number, T is temperature (degrees), and a is the thermal diffusion coefficient (m^2/s).

Assuming that u, v, and p at an arbitrary time t are known, calculating v, u, and p after an infinitesimal time of Δt s using the fractional step method solves Equation (1) and Equation (2) step-by-step. Subsequently, the obtained velocity was substituted into Equation (3) to calculate the temperature. The fractional step method was used for correction by adding the pressure term after calculating the provisional velocity and excluding the pressure term. Eliminating the pressure term from the Navier–Stokes equation yields Equation (4) (two-dimensional Burger's equation).

$$\frac{\partial V}{\partial t} + u\frac{\partial V}{\partial x} + v\frac{\partial V}{\partial y} = \frac{1}{Re}\left(\frac{\partial^2 u}{\partial x^2} + \frac{\partial^2 v}{\partial y^2}\right) \tag{4}$$

These equations can be decomposed into advection and diffusion equations, and the velocities can be easily calculated using the finite-difference method. Using the obtained velocity as the provisional velocity, Equations (5) and (6) are obtained from the difference between the Navier–Stokes equations with and without the pressure term, as follows:

$$u' = u^* - \frac{\partial p}{\partial x}\Delta t \tag{5}$$

$$v' = v^* - \frac{\partial p}{\partial y}\Delta t \tag{6}$$

where u* and v* are tentative velocities, u' and v' are true velocities corrected by pressure after Δt s.

The true velocities were corrected by pressure in Equations (5) and (6). Equation (7) (Poisson's equation) was obtained by substituting these equations into the continuity equation. In addition, pressure p' after Δt s was obtained by solving this equation using an iterative method (SOR method) until the discrepancy falls within an acceptable error range.

$$\frac{\partial^2 p'}{\partial x^2} + \frac{\partial^2 p'}{\partial y^2} = \frac{1}{\Delta t}\left(\frac{\partial u^*}{\partial x} + \frac{\partial v^*}{\partial y}\right) \tag{7}$$

By substituting the obtained pressure and calculating the Navier–Stokes equation, the velocities u and v after Δt s can be obtained.

The temperature distribution was calculated by substituting the velocity obtained from the above calculations into the conservative scalar equation. Considering the symmetry of the steel plate, the analysis range was 20–100 mm, which was the heating distance in the horizontal direction. The mesh size was 0.1 mm^2, Δt was 0.02 s, u, v, and p, at time 0 s was set as 0, and the burner flow velocity was provided only to the part adjacent to the port.

3.2 Analysis Result

The position at which the temperature was at its maximum and the distribution tendency of the temperature were calculated. Under this analysis condition, the

maximum temperature was observed at approximately 22 mm from the center of the steel plate. Figure 3 shows the temperature distributions obtained from the experiment at 1 and 6s from the start of heating. Thermal fluid analysis showed the temperature distribution directly above the steel plate (front surface) exposed to the gas flame. The maximum temperature could not be compared because the temperature on the back side of the steel plate was measured in the experiment. The distance was approximately 22 mm from the center of the steel plate, which agrees with the thermal fluid analysis results. This position corresponds to the maximum point of the aforementioned heat-flux distribution.

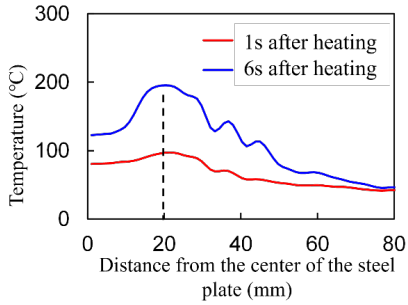

Figure 3
Temperature distributions obtained by the experiment from a 9-mm-thick specimen

4 Thermal Elastic–Plastic Analysis

4.1 Analysis Model

The heating experiment was simulated using thermal elastic–plastic analysis based on the finite element method. Temperature–displacement coupled analysis was performed using the commercial software ABAQUS. The entire specimen was modeled using 4-node shell elements. The temperature dependence of the mechanical properties and physical constants of the materials (Figure 4) was determined by referring to previous literature [12] [13]. The heat transfer from the model surfaces into the air was considered as the thermal boundary condition. Fixing the rigid-body displacement was considered as the mechanical boundary condition.

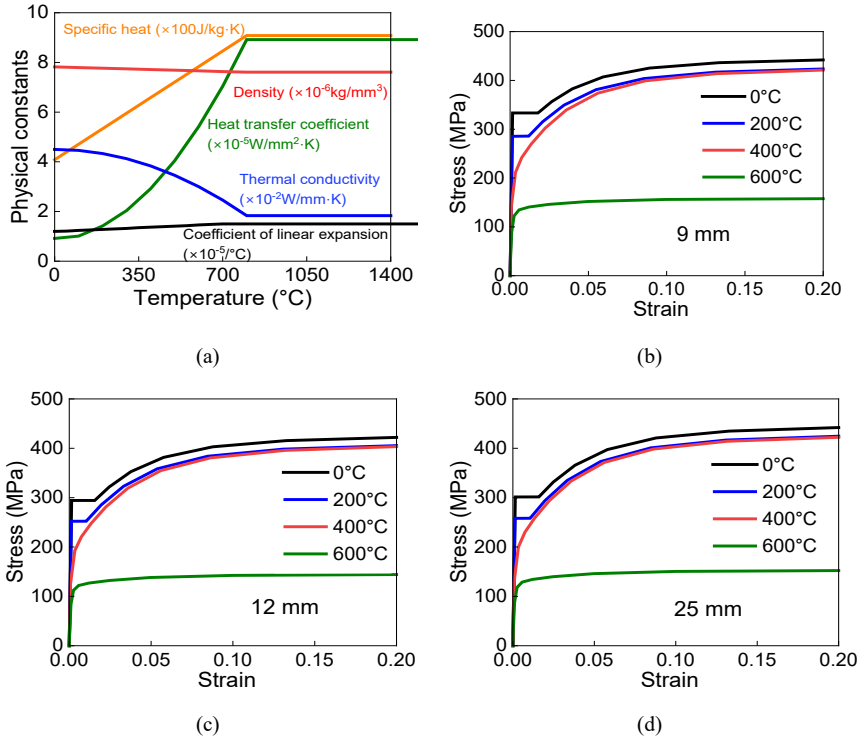

Figure 4

(a) Temperature-dependent physical constants and stress–strain relationships for (b) 9-mm-thick specimens, (c) 12-mm-thick specimens, (d) 25-mm-thick specimens

To construct a simple heat input model, the area affected by the heat input of the gas flame was examined based on the state of the jet flow during heating (Figure 2) and the specimen surface after heating (Figure 5).

Figure 6 shows the analysis model and heat input regions. The heat flux from the gas flame to the steel plate had a maximum value of 22 mm from the center of the steel plate. The heat flux then tended to decrease in proportion to distance. Based on this tendency, the area affected by the heat input was divided into two parts: the region directly affected by the jet, and the region affected by the jet that collided with the steel plate and diffused (diffusion region).

Furthermore, because the structure of a gas flame consists of inner and outer flames that generate a circulating airflow, the part that directly receives the jet was divided into inner and outer flames. The size of each part (the radius of the circle) was determined by referring to the surface of the steel plate after heating (Figure 5). The heat input (surface heat flux) was normally distributed in each part. However, in this analysis, for simplicity, the magnitude of the surface heat flux given to each

part (central inner flame area, q_1; maximum inner flame region, q_2, outer flame region, q_3; and diffusion region, q_4) were set as constants. The surface heat flux values were adjusted such that the temperature history obtained from the experiment could be reproduced. The diffusion radius r_4 of the heat-input-affected region was determined as 74 mm according to the experimental conditions. Radius r_3 was an intermediate value between r_4 and r_2.


Thickness: 9 mm

Figure 5
The surface of the steel plate after heating

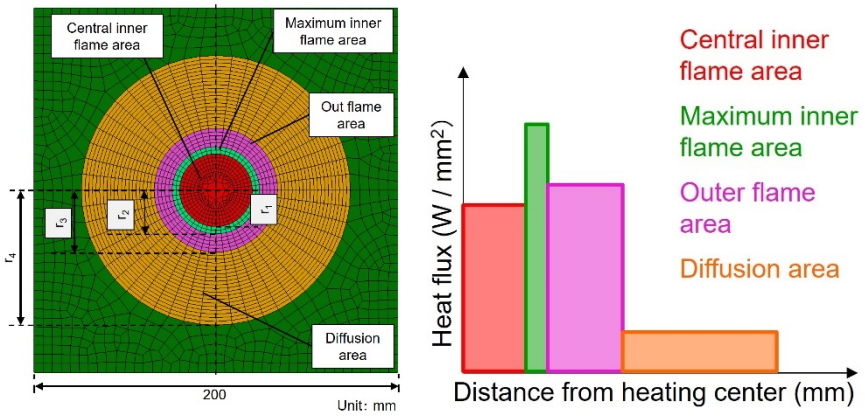

(a) (b)

Figure 6
(a) Analysis model with heated regions and (b) heat flux distribution

4.2 Experimental and Analytical Results

4.2.1 Temperature History

Figure 7 plots the temperature histories at the center of the back surfaces of the specimens during heating measured by the infrared camera (x = 10, 24, 35 (mm)) and the temperature history at a position 50 mm away from the center (x = 50 (mm)) of the back surface of the specimen during heating and cooling measured by the thermocouple. As two specimens were used for each thickness, the average value and range were obtained and are shown in the figure. The solid line in Figure 7 shows the analysis results using the proposed heat input model. By applying the heat input of 0.7 W/mm^2 to the central inner flame region, 1.5 W/mm^2 to the maximum inner flame region, 0.6 W/mm^2 to the outer flame region, and 0.15 W/mm^2 to the diffusion region, the experimental results could be reproduced for each plate thickness. The surface temperature at the heat input position in the analysis was 574.4 °C, which was confirmed within the target temperature range (500–600 °C) in the experiment.

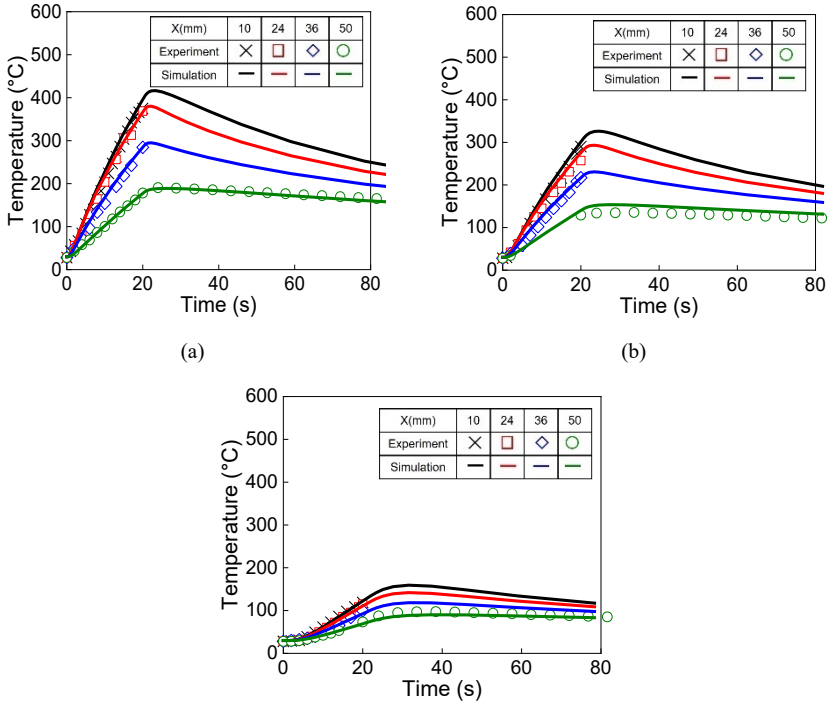

(a) (b)

(c)

Figure 7

Temperature histories of (a) 9-mm thick, (b) 12-mm thick, and (c) 25-mm thick steel plates

4.2.2 Out-of-Plane Deformation

Figure 8 shows the measured results of the out-of-plane deformation and the simulated results of the analysis. For each specimen thickness, the averages of the measurements of the two specimens were used as the experimental results. The tendency of out-of-plane deformation obtained from the experiment for each plate thickness was reproduced by the analysis. The out-of-plane deformation increased with a thinner plate, and all the specimens tended to be convex on the front surface side, heated directly by the gas flame. During the heating process, the temperature of the front surface was higher than that of the back surface, resulting in a greater thermal expansion. During the cooling process, the temperature difference between the front and back surfaces, i.e., the difference in shrinkage between the front and back surfaces, decreased. It was presumed that the thermal expansion on the front surface during heating became dominant, and the front surface deformed into a convex shape.

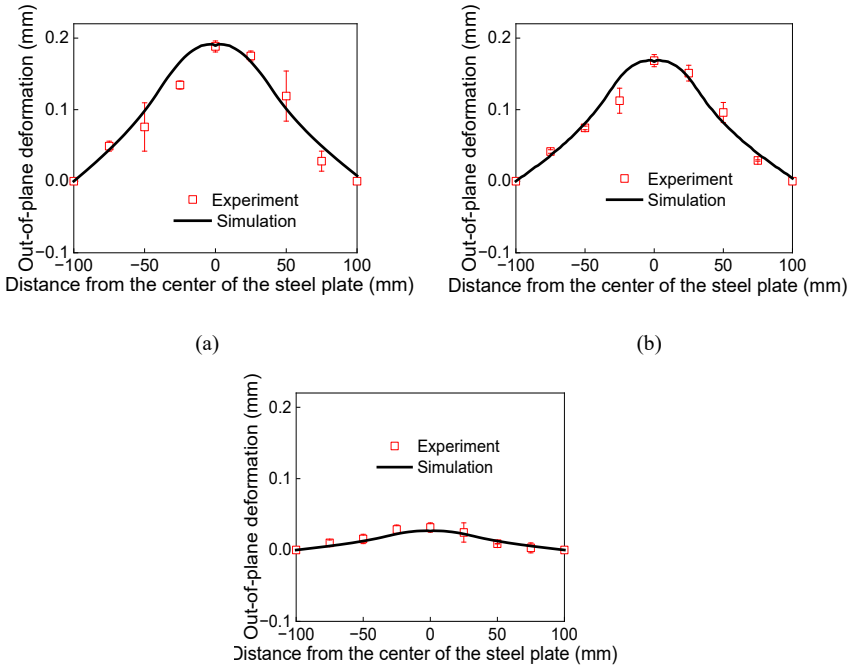

Figure 8
Out-of-plane deformations of (a) 9-mm thick, (b) 12-mm thick, and (c) 25-mm thick steel plates

4.2.3 Residual Stress

Figure 9 shows the measurement results of the residual stress and the results of reproduction by the analysis. The residual stress on the nonheated (back) surface was measured through X-ray diffraction because the metal structure at the directly heated surface affected the measurement accuracy. The average values of the residual stress of the two specimens for each thickness were measured using the experimental results shown in Figure 9. The tendency of the residual stress obtained experimentally for each plate thickness was reproduced by the analysis. The residual stress decreased with increasing plate thickness because the temperature at the back surface decreased with increasing plate thickness.

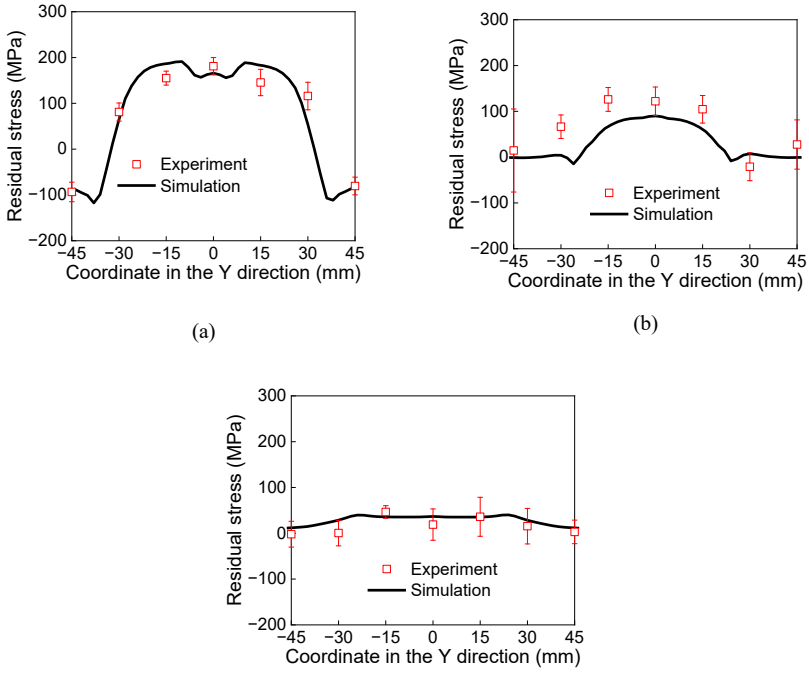

Figure 9
Residual stresses of (a) 9-mm thick, (b) 12-mm thick, and (c) 25-mm thick steel plates

5 Case Study

5.1 Specimen and Experimental Procedure

To investigate the applicability of the proposed heat input model, a heating correction experiment and simulation were performed on a T-shaped welded joint specimen as a case study. A T-shaped joint was fabricated using gas metal arc welding. Figure 10 shows the shapes and dimensions of the specimens. The base plate was square, with the side measuring 250 mm. A rib plate of height 80mm was welded to the midspan of the base plate. The thicknesses of the plates were 9 and 12 mm. The material used for the rib plate was SM400A with different thicknesses. Table 2, lists the mechanical properties of the materials, including yield stress, tensile strength, and elongation, as illustrated in the mill test reports. The out-of-plane welding deformation, was measured at the midspan of the specimen crossing the weld line.

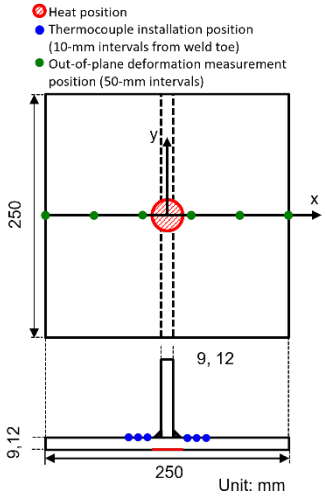

Figure 10
Shape and dimension of T-joint fillet-welded specimens

Figure 11
Image of the heating experiment on the T-joint specimen

Table 2
Mechanical properties of materials for the T-joint fillet-welded specimens

Thickness (mm)	Yield strength (N/mm^2)	Tensile strength (N/mm^2)	Elongation (%)
9	355	463	30
12	353	471	28

The heating experiment was conducted with the target temperature of the heated surface of the base plate ranging from 500 to 600 °C, wherein the rib plate was not welded. Propane and oxygen were used as the gases to heat the specimens. The distance between the specimen and the burner port was 30 mm, the flame length was 60 mm, and the gas flame temperature was 1,500 to 1,800 °C. The distance between the steel plate and the burner port was 20 mm, and heating was performed for 7–8 s. After heating, natural cooling was performed.

Thermocouples were installed on both sides of the weld toe to measure the temperature history of the specimens (Figure 10). There was a 10-mm spacing between every pair of thermocouples. The thermocouple closest to the weld toe was located 10 mm from the weld toe. Figure 11 shows the installation and experimental conditions of the specimens. Out-of-plane deformation was measured before and after heating along the centerline, as shown in Figure 10.

5.2 Numerical Simulation Procedure

The heating correction experiment of the T-joint specimen was simulated via thermal elastic–plastic analysis using the proposed heat input method. The basic analysis conditions were identical to those used for the steel plates. Figure 12 shows the analysis model with 4-node shell elements. Based on the experimental results, the welding out-of-plane deformation was considered as the initial deformation of the model.

The heating region was divided into four regions based on the proposed heat input model. The radius of each region was determined (r_1, r_2, r_3, r_4 = 12, 16, 42, and 74 mm) as per the thermal fluid analysis with heating conditions (heating distance of 30 mm and flame length of 60 mm). The magnitude of the heat flux in each region was examined to reproduce the experimentally-obtained temperature histories.

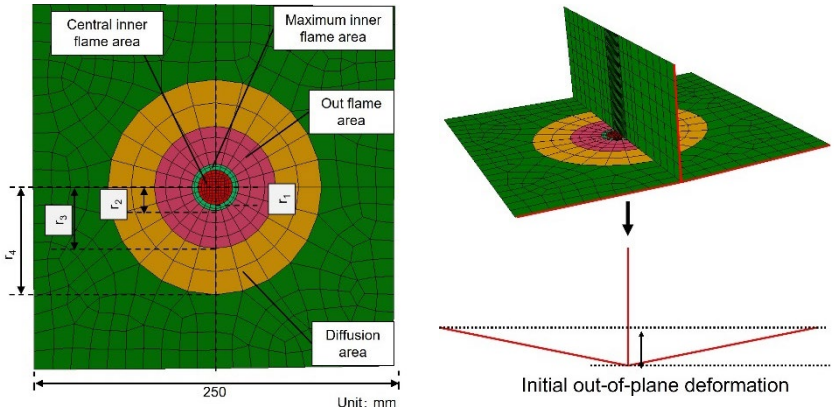

Figure 12
Analysis model for the T-joint specimen

5.3 Results and Discussion

Figure 13 shows the temperature histories obtained from the experiments and analysis. As the measurement results for each thickness of the two specimens showed little variation, only one of the data points for each is shown. This analysis was repeated to reproduce the experimental results by varying the heat flux magnitude. Finally, the experimental temperature history was reproduced using the magnitude of the heat flux as q_1: q_2: q_3: q_4 = 1.8:2.2:1.5:0.7 (W/mm^2). Figure 14, shows the out-of-plane deformations obtained from the experiments and analyses. The correction effect of the out-of-plane deformation in the experiment was reproduced in the analysis. Thus, the heat input model proposed in this study is applicable even to T-shaped welded joints.

It was natural that the smaller the plate thickness of the base plate, the greater the change in corrected out-of-plane deformations when the applied heat input was uniform. The magnitude of the corrected out-of-plane deformation for the 9 mm-thick T-joint specimen was larger than that for the 12 mm-thick T-joint specimen in the experiment. However, this tendency was not observed in the simulation results. The simulation result of the amount of out-of-plane deformation for the 9 mm-thick T-joint model was a little greater than that for the 12 mm-thick T-joint model. The reason might be that the T-joint model was built without initial residual stress. The initial residual stress will affect the results of the amount of out-of-plane deformation. In the future, the model with initial residual stress will be built for further verification.

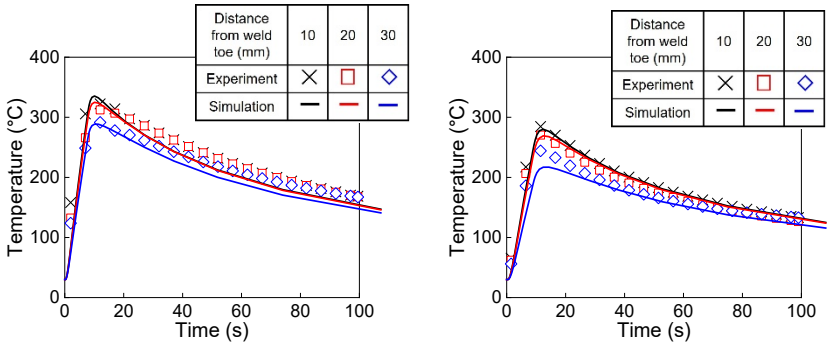

(a) (b)

Figure 13
Temperature histories for T-joint specimen of (a) 9 mm thickness and (b) 12 mm thickness

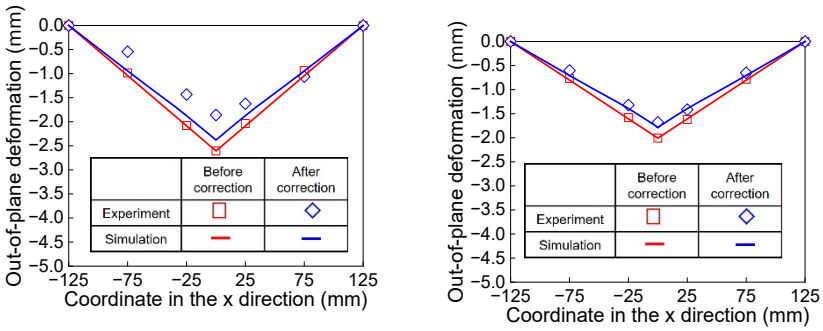

Figure 14

Out-of-plane deformations for the (a) 9-mm thick and (b) 12-mm thick T-joint specimens

Conclusions

In this study, a series of experiments and numerical simulations were performed to propose a simple heat input model for the heating correction of the welding deformation of steel plate members, by Finite Element Analysis (FEM). The main findings of this study are as follows:

(1) The characteristics of the heat input distribution of a gas flame were investigated through a heating experiment on steel plate specimens and thermal fluid analysis. Based on these, a heat input model was developed that provided different surface heat fluxes by dividing the heat input region into four types: inner flame region, maximum region, outer flame region, and diffusion region.

(2) To confirm the validity of the heat input model, a heating experiment was simulated using a thermal elastic–plastic analysis. The temperature history, out-of-plane deformation, and residual stress in the experiment were measured by applying heat to three different thicknesses with the target temperature of the heating surface ranging from 500 to 600 °C. The experimental results could be reproduced through analysis using the proposed heat input model.

(3) To examine the applicability of the proposed heat input model, experiments were conducted on fillet-welded T-section specimens. The temperature history owing to the heating correction and correction effect of the welding deformation could be reproduced by the analysis.

In this study, a thermal fluid analysis was performed, according to the heating conditions and a method was presented to determine the heat input distribution shape. However, because the magnitude of the heat flux for the heat input

distribution shape was determined based on the experimental results, its validity is limited and its generality has not been fully discussed.

For the actual application of this model, it is necessary to conduct a parametric study has to be conducted under various heat input conditions. Future work, to verify the general applicability of the heating correction model, experiments and analyses using larger specimens, with welding deformation, will be conducted.

Acknowledgment

A part of this study was supported by a grant from the Japanese Society of Steel Construction (JSSC).

References

[1] Seong W J, Na S J: Systematization of heat straightening process of stiffened plate by surface flattening. Journal of Materials Processing Technology, 2022, 299: 117333

[2] Gyura L, Gáspár M, Balogh A: The effect of flame straightening on the microstructure and mechanical properties of different strength steels. Welding in the World, 2021, 65(3): 543-560

[3] Seong W J, Jeon Y C, Na S J: Ship-hull plate forming of saddle shape by geometrical approach. Journal of Materials Processing Technology, 2013, 213(11): 1885-1893

[4] Shin J G, Woo J H: Analysis of heat transfer between the gas torch and the plate for the application of line heating. J. Manuf. Sci. Eng., 2003, 125(4): 794-800

[5] Ferreño D, Carral J P, Calderón R L, et al.: Development and experimental validation of a simplified Finite Element methodology to simulate the response of steel beams subjected to flame straightening. Construction and Building Materials, 2017, 137: 535-547

[6] Tokumaru Y, Hirohata M, Mukawa S, et al.: A proposal of simulation method for heating correction of welded members. Proceedings of Constructional Steel. 2020, 28, 731-738 (in Japanese)

[7] Japan Road Association: Specifications for Highway Bridges (II) Steel Members Edition. 2017 (in Japanese)

[8] Kumada M, Nakatogawa T, Hirata K: Heat and mass transfer by Impinging Jet. Journal of Japan Society of Mechanical Engineers.1973, 76, 822-830 (in Japanese)

[9] Okano S, Tsuji H, Mochizuki M: Temperature distribution effect on relation between welding heat input and angular distortion. Science and Technology of Welding and Joining, 2017, 22(1): 59-65

[10] Tomita Y, Hashimoto K, Osawa N, et al.: Study on approximate analysis of convective heat transfer during line-heating process. Journal of the Society of Naval Architects of Japan. 1998, 184, 465-472 (in Japanese)

[11] Cotta R M, Lisboa K M, Curi M F, et al.: A review of hybrid integral transform solutions in fluid flow problems with heat or mass transfer and under Navier–Stokes equations formulation. Numerical Heat Transfer, Part B: Fundamentals, 2019, 76(2): 60-87

[12] Kim Y, Lee J, Inose K: The high accurate prediction of welding distortion generated by fillet welding. Quarterly journal of the Japan welding society. 2005, 23(3), 431-435 (in Japanese)

[13] Nakagawa H, Suzuki H: Ultimate temperatures of steel beams subjected to fire. Steel construction engineering. 1999, 6(22), 57-65 (in Japanese)